JACS
JOURNAL OF THE AMERICAN CHEMICAL SOCIETY
Cite This: J. Am. Chem. Soc. 2019, 141, 9444−9447
Communication
pubs.acs.org/JACS

Conversion of Ethanol via C−C Splitting on Noble Metal Surfaces in Room-Temperature Liquid-Phase

Guangxing Yang,[†,‡] Lida Farsi,[§] Yuhan Mei,[§] Xing Xu,[∥] Anyin Li,[∥] N. Aaron Deskins,[§] and Xiaowei Teng*[,†]

[†]Department of Chemical Engineering, University of New Hampshire, Durham, New Hampshire 03824, United States
[‡]School of Chemistry and Chemical Engineering, South China University of Technology, Guangzhou, Guangdong 510640, China
[§]Department of Chemical Engineering, Worcester Polytechnic Institute, Worcester, Massachusetts 01609, United States
[∥]Department of Chemistry, University of New Hampshire, Durham, New Hampshire 03824, United States

Supporting Information

ABSTRACT: Rh-catalyzed decomposition of ethanol into CO_2 and CH_4 via C−C bond splitting is reported in room-temperature liquid phase under atmospheric pressure. Mechanistic investigations show that C−C bond splitting of ethanol on the noble metal surface is rapid, and CO_2 forms through the oxidation of α-CH_xO and β-CH_x fragments after C−C bond splitting, while CH_4 forms through the hydrogenation of β-CH_x utilizing H atoms from −OH, β-CH_x, and α-CH_xOH fragments.

Activation and splitting of the C−C bond is an important step in the conversion of primary alcohols especially ethanol for producing hydrogen via catalytic process or electricity via 12-electron-transfer electrochemical process. However, these processes are mostly conducted in high vacuum (~10^{-7} Pa) or high temperature (>550 °C) gas phase, high pressure/temperature liquid phase, or in electrochemical systems.[1−10] There are considerable efforts on liquid-phase conversion of alcohols at mild conditions since the explorative work by Cole-Hamilton.[11,12] Beller's group developed molecular complexes to decompose methanol into CO_2 and H_2 at low temperatures (65−95 °C) under ambient pressure.[13−15] Intensive efforts have been devoted to developing heterogeneous catalysts for ethanol dissociation in the liquid-phase in the presence of water and/or oxygen gas. Christensen et al. reported the oxidation of ethanol into acetic acid using Au catalysts at 100−200 °C with oxygen gas.[16,17] Sapi et al. reported that, with oxygen at 60 °C, Pt nanoparticles (2 to 6 nm) were able to catalyze the C−C bond splitting of ethanol to form CO_2, while acetaldehyde (CH_3CHO) was still the main product.[18]

Extensive theoretical work has also been carried out studying ethanol dissociation in the presence of water on various noble metal surfaces with mixed understanding of the reaction pathways. Some work suggested that ethanol decomposition was limited by the C−C bond splitting on Pt (111) surface,[10,19] while the dehydrogenation of the β-C−H bond of ethanol became the rate-determining step on the Rh(111) surface.[20] Hu's group studied ethanol decomposition on various platinum-group-metal surfaces and concluded that ethanol decomposition was not limited by C−C splitting or dehydrogenation, but instead by the removal of *CO species that were reaction intermediates after C−C splitting. Among all the catalysts studied, the Pt (111) surface was found to be the best catalyst for the formation of CO_2.[21,22]

Despite the significant progress in understanding ethanol conversion in aqueous phase, the rate-determining step and the reaction pathways for the complete dissociation of ethanol are still under debate. This may be attributed to the complexity of the reaction environment that involves ethanol, water, and/or oxygen gas. We envisioned that considering ethanol conversion on the surface of noble metal nanoparticles without the presence of water and oxygen, a much less complicated system, would possibly unravel the reaction pathways and clarify the rate-determining step of liquid phase ethanol conversion.

It is known that PtRh-based catalysts are active for electrochemical conversion of ethanol via C−C bond splitting, where the Rh plays a critical role in promoting β-hydrogenation of ethanol, and thus decreasing the energy barrier of C−C splitting with a decreased onset potential for CO_2 generation.[23,24] Based on the success of Rh for the electrochemical conversion of ethanol, we hypothesize that Rh nanoparticles could be used as catalysts for complete decomposition of ethanol to C1 species via C−C splitting without water and/or oxygen gas. Notably, there are no reports of complete splitting of the C−C bond of ethanol using Rh or any other noble metal catalysts in room-temperature liquid-phase without an electrical field.

To investigate the feasibility of our hypothesis, we studied the decomposition of liquid ethanol at room temperature using carbon supported Rh nanoparticles with an average size of 2.1 ± 0.5 nm (Figure S1). Carbon was chosen as the support since it was inert toward ethanol decomposition (Figure S2). The reaction was carried in a batch reactor under an argon atmosphere at 25 °C atmospheric pressure. Gas phase products were drawn from the reactor headspace and analyzed by GC−MS, where rapid production of CH_4 and CO_2 was observed in the first 30 min of the reaction with initial turnover frequencies of 68.6 and 8.7 h^{-1}, respectively (Figures 1a and S3). After that, only minor gas product was observed, indicating the quick deactivation of the catalyst. The deactivated catalyst can be easily regenerated (see Supporting Information). The CH_4 and

Received: December 11, 2018
Published: May 31, 2019

DOI: 10.1021/jacs.8b13115
J. Am. Chem. Soc. 2019, 141, 9444−9447

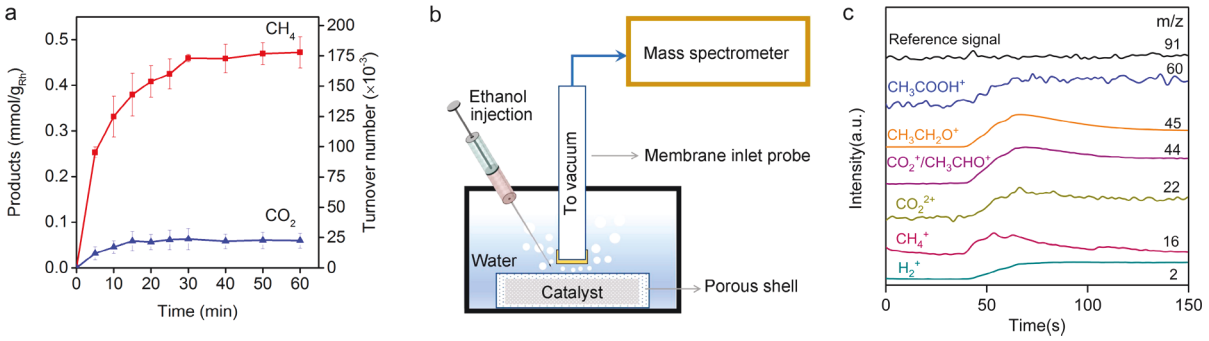

Figure 1. Liquid phase conversion of ethanol using Rh/C catalyst. (a) CO_2 and CH_4 generation. (b,c) Liquid-phase product analysis using online MIMS.

CO_2 generation remained constant, and the Rh catalysts remained unchanged after five cycles of regeneration (Figures S1d and S4). An online membrane inlet mass spectrometer (MIMS) was used to detect liquid-phase products on the surfaces of the catalysts (Figure 1c), showing various chemicals with different mass to charge (m/z) ratios such as acetic acid, acetaldehyde, carbon dioxide, methane, and hydrogen. It is notable that an ethanol and water mixture was used for the MIMS measurement due to poor stability of the membrane in pure ethanol.

A mass spectrometer coupled with electrospray ionization was used to analyze acetaldehyde and acetic acid (Figures S5–S9). Acetaldehyde was derivatized and detected with intensities not significantly higher (2.25 ppm) than the blank ethanol solutions (Table S1). Acetic acid was detected in the negative mode with intensities not significantly higher than the blank ethanol solutions. Similarly, only trace amount of hydrogen gas was detected by MIMS, while GC–MS analysis showed that the most predominant products during reaction were CH_4 and CO_2 (Figure S10). Our results suggest nearly complete dissociation of ethanol via C–C splitting.

In situ attenuated total reflection-Fourier transform infrared spectroscopy (ATR-FTIR) was used to examine the species formed on Rh surface during the reaction (Figures 2a and S11).

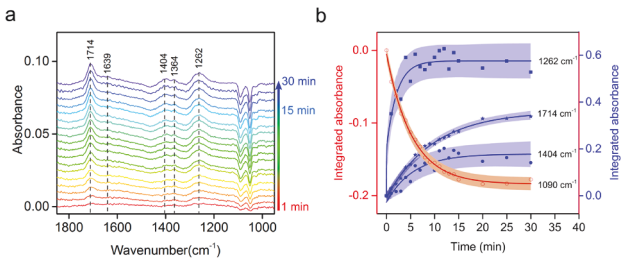

Figure 2. (a) *In situ* ATR-FTIR spectra during the ethanol decomposition. The peak assignment can be found in Figure S5 and Table S2. (b) Integrated absorbance of ethanol, *COH residue, acetic acid or acetaldehyde, and *OCO stretching as functions of reaction time.

The *COH residue (1262 cm^{-1}) confirmed the complete C–C bond splitting, and the negative-going peaks at 1050 and 1090 cm^{-1} can be assigned to ethanol consumption. The formation of acetaldehyde and acetic acid was confirmed by the C=O stretching (1714 and 1639 cm^{-1})[25] and the *OCO stretching (1404 cm^{-1}) from the adsorbed acetate via two oxygen atoms touching the Rh surface.[26] Figure 2b shows the time-resolved integrated absorbance showing a fast consumption of ethanol and rapid accumulations of products from complete (*COH residue) and incomplete (acetate, acetaldehyde, or acetic acid) processes. The accumulation of *COH in Figure 2b showed a similar line shape with the generation of CH_4 and CO_2 in Figure 1a, suggesting that *COH could block the surface and lead to catalysts deactivation. This indicates that C–C bond splitting on the Rh surface is rapid, while the removal of C_1 species from the catalyst surface seems sluggish. Notably, *CH_x residues (2950 cm^{-1}) were also observed (Figure S12), possibly resulting from C–O and C–C cleavages.

We also studied the decomposition of isotope-labeled ethanol to understand the reaction pathways proposed in Figure S13. First, $CH_3{}^{13}CH_2OH$ was used to determine the origin of the C atoms in the formation of the final products. Table 1 shows one

Table 1. C–C Splitting of ^{13}C and D-Labeled Ethanol[a]

$CH_3{}^{13}CH_2OH \rightarrow CH_4 + {}^{13}CO_2 + CO_2$ Eq. 1
$CH_3CH_2OD \rightarrow CH_3D + CO_2$ Eq. 2
$CD_3CH_2OH \rightarrow CD_3H + CD_4 + CD_2H_2 + CO_2$ Eq. 3
$CD_3CD_2OD + CH_3CH_2OH \rightarrow CH_4 + CD_4 + CH_3D + CHD_3 + CH_2D_2$ Eq. 4

Products (%)	Isotope-labeled Reactants			
	$CH_3{}^{13}CH_2OH$	CH_3CH_2OD	CD_3CH_2OH	CD_3CD_2OD CH_3CH_2OH
$^{12}CO_2$	54.0	~ 100	100	100
$^{13}CO_2$	46.0	/	/	/
$^{13}CH_4$	/	/	/	/
CH_4	~100	94.4	/	69.9
CH_3D	/	5.6	/	8.2
CH_2D_2	/	/	18.0	3.9
CHD_3	/	/	71.8	8.2
CD_4	/	/	10.1	9.9

[a]10 mg Rh/C catalysts (10 wt % Rh), 0.3 mL of isotope-labeled ethanol, 25 °C and normal atmospheric pressure, 1 h reaction under magnetic stirring.

form of CH_4 ($^{12}CH_4$) and two forms of CO_2 (54% $^{12}CO_2$ and 46% $^{13}CO_2$) detected (Figure S14), suggesting that α- and β-carbons equally contributed to the CO_2 formation. Since two oxygen atoms must come from separate ethanol molecules, this result indicated an intermolecular reaction during ethanol decomposition. Moreover, the absence of $^{13}CH_4$ indicated that hydrogenation of α-CH_X to CH_4 is unlikely (although α-C–O bond cleavage must occur in order to provide oxygen atoms for CO_2 formation), and only β-CH_X participates in the formation of CH_4. However, it is possible that some α-^{13}C fragments might

DOI: 10.1021/jacs.8b13115
J. Am. Chem. Soc. 2019, 141, 9444–9447

exist on catalyst surface and/or in solution in the forms of C2 (acetic acid and/or acetaldehyde) and C1 product (*CHO) due to the incomplete ethanol conversion.

To understand CH_4 formation, three types of ethanol reagents (CH_3CH_2OD, CD_3CH_2OH, and CD_3CD_2OD) were used to determine the partition of H atoms from hydroxyl (−OH), methanediyl ($-CH_2-$), and methyl ($-CH_3$) groups. Table 1 shows that the decomposition of CH_3CH_2OD yielded CH_4 (94.4%) and CH_3D (5.6%). Fewer CH_3D suggested that formation of CH_4 via combining a methyl group ($-CH_3$) with a D atom from an −OD group is less favorable. We postulate that though O−H cleavage is facile (as density functional theory (DFT) calculations show in Figure 3), H from $-CH_2-$

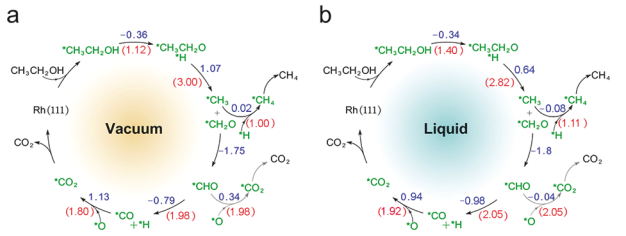

Figure 3. DFT calculations conducted in (a) vacuum and (b) liquid ethanol for the ethanol decomposition. Blue numbers are reaction energies, and red numbers are activation energies (all in eV).

dehydrogenation is also facile and more available for $*CH_3$ to produce CH_4. This argument is also supported by isotope experiments, which indicated a very dynamic H movement even between intermolecular C−H fragments. Therefore, after the C−C bond is cleaved, the resulting $-CH_3$ group quickly combines with an H atom from CH_X fragments to form CH_4.[27] The decomposition of CD_3CH_2OH yielded CD_4, CD_3H, and CH_2D_2 (Figure S15). The major form of methane was CD_3H, suggesting that combining a $-CH_3$ group with an H atom from the $-CH_2-$ group is favorable since an H atom from the −OH group made a minor contribution to CH_4 formation. A relatively large amount of CH_2D_2 (18%) was observed, implying that a $-CH_3$ moiety easily dehydrogenated and recombined with an H atom from the $-CH_2-$ group to form CH_4 since β-carbon from the $-CD_3$ group is the only source of CH_4. Formation of CD_4 suggested that a $-CD_3$ moiety can combine with a D atom from the $-CD_3$ of a neighboring ethanol, direct evidence of an intermolecular reaction. When equal amounts of CD_3CD_2OD and CH_3CH_2OH were used, all forms of methane were detected (Table 1), again suggesting an intermolecular reaction. The high concentration of CH_4 compared to CD_4 indicates that the deuteration of the methane produces a primary kinetic isotope effect (k_H/k_D = 69.9%/9.9% = 7),[28] where CH_4 formation is limited by the combination between $-CH_3$ and the H atom from $-CH_2-$ moiety.

Figure 3 shows the DFT calculations of catalytic cycles for ethanol decomposition on Rh(111) surfaces in vacuum and liquid conditions. More details are shown in Figures S16−S20. Among the major catalytic steps in liquid ($*CH_3CH_2OH \rightarrow *CH_3CH_2O \rightarrow *CH_3 + *OCH_2 \rightarrow *CH_4 + *CO_2$), the reaction energy for C−C breaking ($*CH_3CH_2O \rightarrow *CH_3 + *OCH_2$) is the highest (0.64 eV). This suggests C−C splitting remains mechanistically difficult during liquid-phase ethanol decomposition. Notably, reaction energies of each catalytic step are lowered (or at least comparable) in liquid compared to in vacuum. Especially the reaction energy for C−C breaking is significantly lower in liquid (0.64 eV) compared to in vacuum (1.07 eV). We also modeled C−C breaking in $*CH_3CO$ and $*CH_2CO$ (key intermediates during ethanol oxidation[19,29]) in vacuum and liquid conditions. C−C breaking energies in liquid were lower due to ethanol interactions compared to vacuum (see Supporting Information), suggesting ethanol decomposition via C−C splitting is more viable in liquid than in vacuum. Notably, the reported room-temperature C−C bond cleavage of ethanol was not unique to pure ethanol, where aqueous ethanol conversion on Rh/C led to the same gas products (CH_4 and CO_2) compared with pure ethanol. This indicates that, in the presence of water, ethanol decomposition may follow similar mechanisms compared to when pure ethanol is used.[30] Finally, we found that ethanol decomposition is not specific to Rh, but also on other noble metals (Figure S22), the activities of which follow Rh ≈ Pt > Ir ≫ Au ≈ Ag. The reaction energies of C−C splitting on (111) surfaces of various metals were calculated in vacuum (Figures S23−S26). Three precursors ($*CH_3CO$, $*CH_2CO$, and *CHCO) were considered, where Au and Ag have much higher reaction energy for C−C splitting and are inactive for ethanol decomposition.

In summary, we report room-temperature liquid-phase conversion of ethanol into CH_4 and CO_2 via C−C bond splitting. Reported results are different from reforming process,[1,6,8] where ethanol and water can be easily activated at high temperature/pressure for H_2 and CO_2 productions. The reaction pathways were studied using isotope-labeled ethanol. DFT calculations in vacuum and liquid conditions suggested that C−C bond splitting remains mechanistically difficult, but that the reaction energy for C−C breaking is lowered in liquid compared to vacuum. This study provides the understanding of breaking C−C bonds in alcohols or other hydrocarbons via room-temperature liquid-phase reaction using noble metal nanocatalysts.

■ ASSOCIATED CONTENT

Supporting Information

The Supporting Information is available free of charge on the ACS Publications website at DOI: 10.1021/jacs.8b13115.

Material synthesis/characterization and DFT calculations (PDF)

■ AUTHOR INFORMATION

Corresponding Author

*xw.teng@unh.edu

ORCID

N. Aaron Deskins: 0000-0002-0041-7960

Xiaowei Teng: 0000-0001-9547-7175

Notes

The authors declare no competing financial interest.

■ ACKNOWLEDGMENTS

This work was supported by the National Science Foundation (CBET-1159662). Research conducted at the Advanced Photon Source at the Argonne National Laboratory and Center for Functional Nanomaterials at Brookhaven National Laboratory was sponsored by the U.S. Department of Energy.

■ REFERENCES

(1) Sun, J.; Wang, Y. Recent Advances in Catalytic Conversion of Ethanol to Chemicals. *ACS Catal.* **2014**, *4*, 1078−1090.

DOI: 10.1021/jacs.8b13115
J. Am. Chem. Soc. 2019, 141, 9444−9447

(2) Liu, X. Y.; Xu, B. J.; Haubrich, J.; Madix, R. J.; Friend, C. M. Surface-Mediated Self-Coupling of Ethanol on Gold. *J. Am. Chem. Soc.* **2009**, *131*, 5757−5759.
(3) Chen, D. A.; Friend, C. M. Controlling Deoxygenation Selectivity by Surface Modification: Reactions of Ethanol on Oxygen- and Sulfur-Covered Mo(110). *J. Am. Chem. Soc.* **1998**, *120*, 5017−5023.
(4) Shan, J. J.; Janvelyan, N.; Li, H.; Liu, J. L.; Egle, T. M.; Ye, J. C.; Biener, M. M.; Biener, J.; Friend, C. M.; Flytzani-Stephanopoulos, M. Selective Non-Oxidative Dehydrogenation of Ethanol to Acetaldehyde and Hydrogen on Highly Dilute Nicu Alloys. *Appl. Catal., B* **2017**, *205*, 541−550.
(5) Zhou, G.; Barrio, L.; Agnoli, S.; Senanayake, S. D.; Evans, J.; Kubacka, A.; Estrella, M.; Hanson, J. C.; Martinez-Arias, A.; Fernandez-Garcia, M.; Rodriguez, J. A. High Activity of $Ce_{1-X}ni_xo_{2-Y}$ for H_2 Production through Ethanol Steam Reforming: Tuning Catalytic Performance through Metal-Oxide Interactions. *Angew. Chem., Int. Ed.* **2010**, *49*, 9680−9684.
(6) Deluga, G. A.; Salge, J. R.; Schmidt, L. D.; Verykios, X. E. Renewable Hydrogen from Ethanol by Autothermal Reforming. *Science* **2004**, *303*, 993−997.
(7) Mallat, T.; Baiker, A. Oxidation of Alcohols with Molecular Oxygen on Solid Catalysts. *Chem. Rev.* **2004**, *104*, 3037−3058.
(8) Fatsikostas, A. N.; Kondarides, D. I.; Verykios, X. E. Steam Reforming of Biomass-Derived Ethanol for the Production of Hydrogen for Fuel Cell Applications. *Chem. Commun.* **2001**, 851−852.
(9) Wang, L. C.; Stowers, K. J.; Zugic, B.; Personick, M. L.; Biener, M. M.; Biener, J.; Friend, C. M.; Madix, R. J. Exploiting Basic Principles to Control the Selectivity of the Vapor Phase Catalytic Oxidative Cross-Coupling of Primary Alcohols over Nanoporous Gold Catalysts. *J. Catal.* **2015**, *329*, 78−86.
(10) Kowal, A.; Li, M.; Shao, M.; Sasaki, K.; Vukmirovic, M. B.; Zhang, J.; Marinkovic, N. S.; Liu, P.; Frenkel, A. I.; Adzic, R. R. Ternary Pt/Rh/Sno_2 Electrocatalysts for Oxidizing Ethanol to Co_2. *Nat. Mater.* **2009**, *8*, 325−330.
(11) Morton, D.; Colehamilton, D. J. Molecular Hydrogen Complexes in Catalysis: Highly Efficient Hydrogen Production from Alcoholic Substrates Catalyzed by Ruthenium Complexes. *J. Chem. Soc., Chem. Commun.* **1988**, 1154−1156.
(12) Morton, D.; Colehamilton, D. J.; Utuk, I. D.; Panequesosa, M.; Lopezpoveda, M. Hydrogen Production from Ethanol Catalyzed by Group-8 Metal Complexes. *J. Chem. Soc., Dalton Trans.* **1989**, 489−495.
(13) Alberico, E.; Sponholz, P.; Cordes, C.; Nielsen, M.; Drexler, H. J.; Baumann, W.; Junge, H.; Beller, M. Selective Hydrogen Production from Methanol with a Defined Iron Pincer Catalyst under Mild Conditions. *Angew. Chem., Int. Ed.* **2013**, *52*, 14162−14166.
(14) Nielsen, M.; Junge, H.; Kammer, A.; Beller, M. Towards a Green Process for Bulk-Scale Synthesis of Ethyl Acetate: Efficient Acceptorless Dehydrogenation of Ethanol. *Angew. Chem., Int. Ed.* **2012**, *51*, 5711−5713.
(15) Nielsen, M.; Alberico, E.; Baumann, W.; Drexler, H. J.; Junge, H.; Gladiali, S.; Beller, M. Low-Temperature Aqueous-Phase Methanol Dehydrogenation to Hydrogen and Carbon Dioxide. *Nature* **2013**, *495*, 85−89.
(16) Christensen, C. H.; Jorgensen, B.; Rass-Hansen, J.; Egeblad, K.; Madsen, R.; Klitgaard, S. K.; Hansen, S. M.; Hansen, M. R.; Andersen, H. C.; Riisager, A. Formation of Acetic Acid by Aqueous-Phase Oxidation of Ethanol with Air in the Presence of a Heterogeneous Gold Catalyst. *Angew. Chem., Int. Ed.* **2006**, *45*, 4648−4651.
(17) Jorgensen, B.; Christiansen, S. E.; Thomsen, M. L. D.; Christensen, C. H. Aerobic Oxidation of Aqueous Ethanol Using Heterogeneous Gold Catalysts: Efficient Routes to Acetic Acid and Ethyl Acetate. *J. Catal.* **2007**, *251*, 332−337.
(18) Sapi, A.; Liu, F. D.; Cai, X. J.; Thompson, C. M.; Wang, H. L.; An, K. J.; Krier, J. M.; Somorjai, G. A. Comparing the Catalytic Oxidation of Ethanol at the Solid-Gas and Solid-Liquid Interfaces over Size-Controlled Pt Nanoparticles: Striking Differences in Kinetics and Mechanism. *Nano Lett.* **2014**, *14*, 6727−6730.
(19) Sutton, J. E.; Vlachos, D. G. Ethanol Activation on Closed-Packed Surfaces. *Ind. Eng. Chem. Res.* **2015**, *54*, 4213−4225.
(20) Choi, Y.; Liu, P. Understanding of Ethanol Decomposition on Rh(111) from Density Functional Theory and Kinetic Monte Carlo Simulations. *Catal. Today* **2011**, *165*, 64−70.
(21) Sheng, T.; Lin, W.-F.; Hardacre, C.; Hu, P. Significance of B-Dehydrogenation in Ethanol Electro-Oxidation on Platinum Doped with Ru, Rh, Pd, Os and Ir. *Phys. Chem. Chem. Phys.* **2014**, *16*, 13248−13254.
(22) Kavanagh, R.; Cao, X.-M.; Lin, W.-F.; Hardacre, C.; Hu, P. Origin of Low Co2 Selectivity on Platinum in the Direct Ethanol Fuel Cell. *Angew. Chem., Int. Ed.* **2012**, *51*, 1572−1575.
(23) Li, M.; Cullen, D. A.; Sasaki, K.; Marinkovic, N. S.; More, K.; Adzic, R. R. Ternary Electrocatalysts for Oxidizing Ethanol to Carbon Dioxide: Making Ir Capable of Splitting C−C Bond. *J. Am. Chem. Soc.* **2013**, *135*, 132−141.
(24) Yang, G.; Namin, L. M.; Aaron Deskins, N.; Teng, X. Influence of *Oh Adsorbates on the Potentiodynamics of the Co_2 Generation During the Electro-Oxidation of Ethanol. *J. Catal.* **2017**, *353*, 335−348.
(25) Shao, M. H.; Adzic, R. R. Electrooxidation of Ethanol on a Pt Electrode in Acid Solutions: In Situ Atr-Seiras Study. *Electrochim. Acta* **2005**, *50*, 2415−2422.
(26) Iwasita, T.; Nart, F. C.; Lopez, B.; Vielstich, W. On the Study of Adsorbed Species at Platinum from Methanol, Formic Acid and Reduced Carbon Dioxide Via in Situ Ftir Spectroscopy. *Electrochim. Acta* **1992**, *37*, 2361−2367.
(27) Vesselli, E.; Baraldi, A.; Comelli, G.; Lizzit, S.; Rosei, R. Ethanol Decomposition: C-C Cleavage Selectivity on Rh(111). *ChemPhysChem* **2004**, *5*, 1133−1140.
(28) Westheimer, F. H. The Magnitude of the Primary Kinetic Isotope Effect for Compounds of Hydrogen and Deuterium. *Chem. Rev.* **1961**, *61*, 265−273.
(29) Ferrin, P.; Simonetti, D.; Kandoi, S.; Kunkes, E.; Dumesic, J. A.; Norskov, J. K.; Mavrikakis, M. Modeling Ethanol Decomposition on Transition Metals: A Combined Application of Scaling and Bronsted-Evans-Polanyi Relations. *J. Am. Chem. Soc.* **2009**, *131*, 5809−5815.
(30) Yang, G.; Charles, D. S.; Deskins, N. A.; Hu, E.; Reinhart, B.; Bai, J.; Frenkel, A. I.; Teng, X. Tuning Selectivity in Catalytic Decomposition of Aqueous Ethanol Using Rh/Rh_2O_3 Mixed Phase Nanoparticles. In Preparation.

DOI: 10.1021/jacs.8b13115
J. Am. Chem. Soc. 2019, 141, 9444−9447